

1 **Reversible and Irreversible H_{AuCl₄} Binding to DNA for Seeded Gold Nanoparticle**
2 **Growth and Opposite DNA and Aptamers Colorimetric Sensing Outcomes**

3 Chang Lu^{1,2}, Mohamad Zandieh², Jinkai Zheng^{1*} and Juewen Liu^{2*}

4 1. Institute of Food Science and Technology, Chinese Academy of Agricultural Sciences,
5 Beijing 100193, P. R. China. Email: zhengjinkai@caas.cn

6 2. Department of Chemistry, Waterloo Institute for Nanotechnology, University of Waterloo,
7 Waterloo, ON, N2L 3G1, Canada. Email: liujw@uwaterloo.ca

8 **Abstract**

9 DNA-directed seeded growth of gold nanoparticles has been used for the development of
10 aptamer-based biosensors with the assumption that target analytes can modulate the
11 adsorption of aptamers to the gold seeds and thus the growth reaction. To understand the
12 reaction, we first examined the effect of single- and double-stranded DNA and found that
13 they had a similar promotion effect of anisotropic growth, suggesting that DNA cannot be
14 detected using this method. By studying the interaction between H_{AuCl₄} and DNA, both
15 weak reversible binding and strong irreversible binding were identified, with the latter
16 became dominating with longer incubation time. Single- and double-stranded DNA had
17 similar weak binding to H_{AuCl₄}, and this weak binding was more important for the growth
18 reaction. We then tested the three aptamers, where only cortisol appeared to modulate its
19 aptamer adsorption and the growth reaction reflected aptamer binding. Hg²⁺ showed no
20 advantage for its aptamer, and quinine induced aggregation of AuNPs and it cannot be
21 detected by this reaction either. Therefore, each aptamer target needs to be individually
22 studied to test if this method is applicable. We also noted that DNA and aptamers have
23 opposite outcomes for the target-dependent growth reactions.

24
25 **Keywords:** DNA, gold, growth, aptamer target, colorimetric sensing

26

1 **Introduction**

2 DNA oligonucleotides can strongly adsorb to gold surfaces, and such adsorption can change
3 the properties of gold nanoparticles (AuNPs) for biosensing applications.¹⁻³ For example, the
4 increased colloidal stability of AuNPs was used for the detection of DNA hybridization, since
5 the adsorption of double-stranded DNA (dsDNA) was slower than single-stranded DNA
6 (ssDNA).^{4, 5} Aggregated AuNPs have a different color, stronger Raman enhancement
7 properties and better photothermal effects, allowing colorimetric, SERS and
8 temperature-based detection.⁶⁻⁸ In addition, DNA can modulate the peroxidase-like catalytic
9 activity of AuNPs,^{9, 10} and AuNP can quench the fluorescence of fluorescently labeled
10 DNA.^{11, 12} In all these cases, it is critical to modulate DNA adsorption using its
11 complementary DNA (cDNA) or aptamer targets.^{13, 14}

12 DNA-directed seeded growth of AuNPs is an interesting reaction, and various DNA
13 sequences have been used to regulate the growth.¹⁵⁻¹⁸ In a typical experiment, a low
14 concentration of gold nanoseeds (AuNSs) are incubated with a DNA oligonucleotide. Then
15 HAuCl₄ is added in the presence of a reducing agent such as NH₂OH.¹⁹⁻²¹ It was perceived
16 that forming dsDNA and aptamer binding complexes would affect the growth process.²²⁻²⁴
17 Fang et al. attached thiolated DNA to AuNSs and observed color transitioned from red to
18 blue with more cDNA added.²² However, no DNA detection was reported using nonthiolated
19 DNA. Aptamer based detection was reported, where aptamer targets were believed to inhibit
20 aptamer adsorption to AuNSs and the seeded growth.^{25, 26} However, none of these works
21 considered potential interactions between target molecules and gold surfaces.²⁷⁻²⁹ Different
22 aptamer targets may interact differently with AuNPs, which in turn affects aptamer
23 adsorption.^{14, 30, 31}

24 In this work, we aimed to understand the fundamental surface interactions during the
25 seeded growth reaction. We first used nonthiolated DNA to direct seeded AuNP growth for
26 cDNA detection. We then studied the interaction between HAuCl₄ and DNA, and identified
27 both reversible weak and irreversible strong interactions, with the former dominating the
28 seeded growth. Finally, we studied the detection of a few aptamer targets, including a metal
29 ion (Hg²⁺) and two small molecules (cortisol and quinine). Our results indicated that the

1 growth of AuNPs cannot be used for the detection of cDNA, whereas the outcome of aptamer
2 targets varied. Unlike other AuNP-based detection methods based on colloidal stability,
3 fluorescence quenching and catalysis, where DNA and aptamer probes were expected to have
4 similar responses, in the seeded growth system, DNA and aptamer targets behaved oppositely.

5 **Materials and Methods**

6 **Chemicals**

7 All of the DNA samples used in this work were purchased from Integrated DNA
8 Technologies (Coralville, IA) and their sequences are listed in Table 1. Potassium cyanide
9 (KCN), hydroxylamine hydrochloride ($\text{NH}_2\text{OH}\cdot\text{HCl}$), gold(III) chloride trihydrate
10 ($\text{HAuCl}_4\cdot 3\text{H}_2\text{O}$), mercury acetate ($\text{Hg}(\text{OAc})_2$), magnesium chloride (MgCl_2), fluorescein
11 sodium salt, cortisol, quinine hemisulfate monohydrate, deoxycholic acid, and 17β -estradiol
12 were from Sigma-Aldrich. Trisodium citrate dihydrate, sodium chloride (NaCl), sodium
13 phosphate monobasic monohydrate, and sodium phosphate dibasic heptahydrate were from
14 Mandel Scientific (Guelph, ON, Canada). SYBR Green I (SGI) was purchased from Lonza
15 (Rockland, ME). AuNSs (13 nm) were synthesized using the citrate reduction method.³²
16 Milli-Q water was used to prepare buffers and solutions.

17 **Growth of AuNPs for DNA detection**

18 4 μL 13 nm AuNSs (12 nM), 154 μL H_2O , 20 μL 1 mM MgCl_2 , and 2 μL 10 μM 24-mer
19 random sequenced DNA (24-mer DNA) were incubated overnight. Then, 20 μL c-24-mer or
20 24-mer DNA with a final concentration of (0 to 100 nM) was added and the samples were
21 heated at 95°C for 1 min and cooled to room temperature gradually over 1 h. 5 μL 400 mM
22 NH_2OH and 20 μL 1.9 mM HAuCl_4 were then sequentially added and reacted for 15 min at
23 room temperature to initiate the seeded growth. Photographs were taken using a digital
24 camera and UV-vis spectra were measured with a microplate reader (Tecan Spark). To
25 confirm successful formation of dsDNA, to 50 μL 100 nM annealed DNA, 1 μL SGI (50 \times),
26 10 μL PB buffer (pH 7.6, 50 mM), and 40 μL H_2O were mixed. The fluorescence emission
27 spectra were measured with the microplate reader (Ex: 490 nm; Em: 520 nm-600 nm).

28

1 **Table 1. The DNA Sequences Used in This Work**

Names	Sequences and modifications (5'–3')
A30	AAAAAAAAAAAAAAAAAAAAAAAAAAAAAAAA
T30	TTTTTTTTTTTTTTTTTTTTTTTTTTTTTT
C30	CCCCCCCCCCCCCCCCCC
Cortisol aptamer (CSS.1)	GACGACGCCCGCATGTTCCATGGATAGTCTTGACTAGTCGTC
Mutated cortisol aptamer (CSS.1-mt)	GACGACACCCGCATGTTCCATGGGTAGTCTTGACTAGTCGTC
Quinine aptamer (MN4)	GGCGACAAGGAAAATCCTTCAACGAAGTGGGTCGCC
c-MN4	GGCGACCCACTTCGTTGAAGGATTTTCCTTGTCGCC
FAM-MN4	GGCGACAAGGAAAATCCTTCAACGAAGTGGGTCGCC-FAM
FAM-24-mer DNA	FAM- ACGCATCTGTGAAGAGAACCTGGG
24-mer DNA	ACGCATCTGTGAAGAGAACCTGGG
c-24-mer DNA	CCCSGGTTCTCTTCACAGATGCGT

2

3 **Interaction of H_{AuCl}₄ with ssDNA and dsDNA**

4 To investigate the order of reagent addition, H_{AuCl}₄ was added in four conditions. (1) 150
5 μL 0.5 nM AuNSs were mixed with 1.5 μL 100 μM DNA (A30/T30/C30) for 15 min,
6 followed by adding 7.5 μL 400 mM NH₂OH and 0.53 μL 50 mM H_{AuCl}₄ sequentially; (2)
7 150 μL 0.5 nM AuNSs were mixed with 1.5 μL 100 μM DNA (A30/T30/C30) for 15 min,
8 followed by adding 0.53 μL 50 mM H_{AuCl}₄ and 7.5 μL 400 mM NH₂OH sequentially; (3)
9 150 μL 0.5 nM AuNSs were mixed with 1.5 μL 100 μM DNA (A30/T30/C30) for 15 min,
10 and then 0.53 μL 50 mM H_{AuCl}₄ was added and incubated for 15 min, followed by adding
11 7.5 μL 400 mM NH₂OH; (4) 143.5 μL H₂O, 0.53 μL 50 mM H_{AuCl}₄ and 1.5 μL 100 μM
12 DNA (A30/T30/C30) were incubation for 15 min, and then 6.47 μL 12 nM AuNSs were
13 added and incubated for 15 min, followed by adding 7.5 μL 400 mM NH₂OH.

14 The interactions of H_{AuCl}₄ with ssDNA and dsDNA were investigated by using
15 FAM-24-mer DNA. 10 μM (final concentration) FAM 24-mer DNA was mixed with 24-mer

1 DNA or c-24-mer DNA in buffer (10 mM PB, 50 mM NaCl, pH 7.6) and annealed as
2 described above. 100 μ L 10 mM PB (pH 7.6) and 1 μ L 10 μ M FAM-24-mer DNA or the
3 annealed DNA were mixed in a microplate and the fluorescence was monitored for 5 min (Ex
4 485 nm; Em 530 nm). Then, 1 μ L 16.7 mM HAuCl₄ was added and the fluorescence was
5 monitored for 35 min. Finally, 2 μ L 1 M KCN was added and the fluorescence was
6 monitored for another 10 min.

7 **Growth of AuNPs for Hg²⁺ detection**

8 150 μ L 12 nM AuNSs and 50 μ L 4 μ M T30 or A30 DNA were incubated overnight, after
9 which 300 μ L Hg²⁺ (final: 0, 5 nM, 25 nM, 50 nM, 250 nM) and 80 μ L 2 mM MgCl₂ were
10 added and incubated at 37°C for 20 min, followed by adding 30 μ L 100 mM NH₂OH and 10
11 μ L 30 mM HAuCl₄. Photographs were taken and UV-vis spectra were measured. To verify
12 the T30-Hg²⁺ binding, 100 μ L PB buffer (pH 7.6, 10 mM), 1 μ L 10 μ M T30 or A30, 2 μ L
13 Hg²⁺, 2 μ L 20 mM MgCl₂ were mixed at 37°C for 30 min, and then 1 μ L SGI (50 \times) was
14 added and the fluorescence emission spectra were collected.

15 **Growth of AuNPs for cortisol and quinine detection**

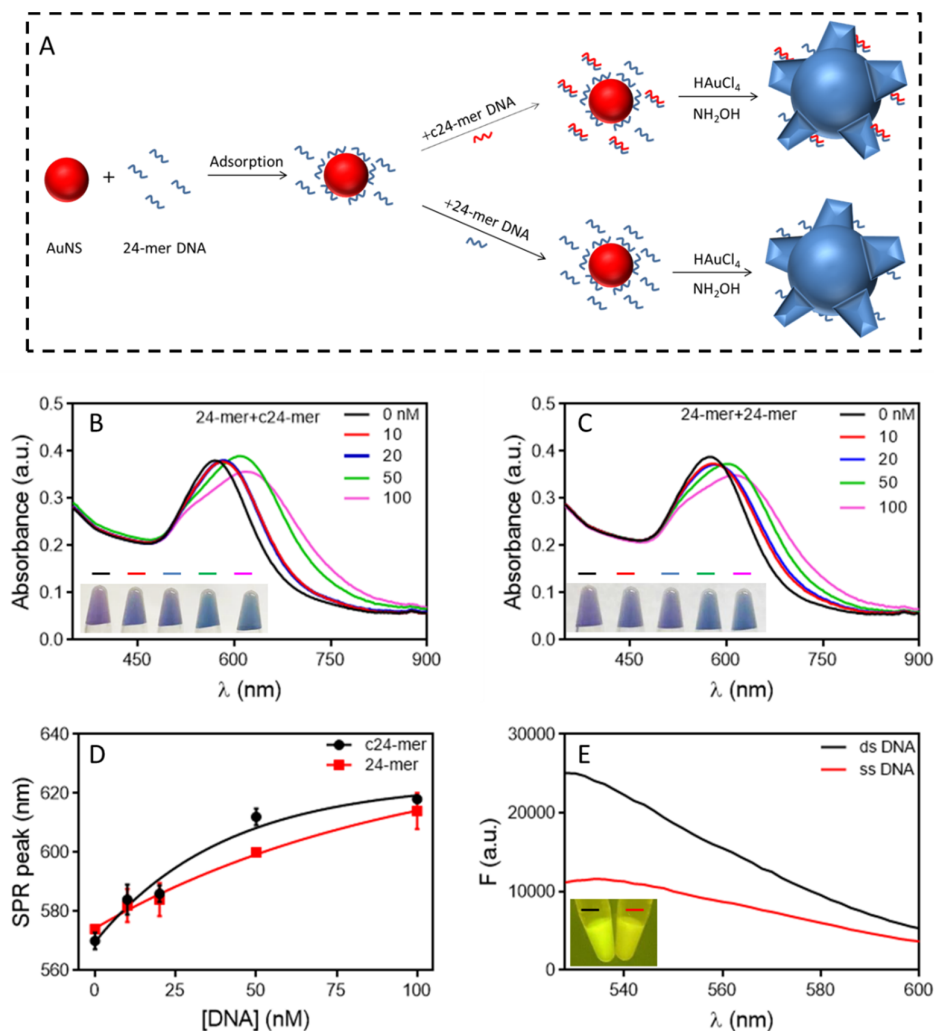
16 For cortisol detection, 4 μ L 12 nM AuNSs, 155 μ L H₂O, 20 μ L 1 mM MgCl₂, and 1 μ L 100
17 μ M CSS.1 or CSS.1-mt were incubated overnight. Afterwards, 20 μ L cortisol (final 0, 0.5 μ M,
18 1 μ M, 2 μ M, 5 μ M, 10 μ M) was mixed with the solution for 40 min. 5 μ L 400 mM NH₂OH
19 and 30 μ L 1.9 mM HAuCl₄ were sequentially added to the solution and reacted for 15 min to
20 initiate the reduction reaction. For quinine detection, 14.3 μ L 12 nM AuNSs, 145.7 μ L H₂O,
21 20 μ L 1 mM MgCl₂, and 0.9 μ L 100 μ M MN4 or c-MN DNA were incubated overnight.
22 After that, 20 μ L cortisol (final 0, 0.5 μ M, 1 μ M, 5 μ M) was mixed with the solution for 40
23 min. 5 μ L 400 mM NH₂OH and 30 μ L 1.9 mM HAuCl₄ were sequentially added into the
24 solution and reacted for 15 min to initiate the reduction reaction. Photographs were taken and
25 UV-vis spectra were measured.

26

27 **Results and Discussion**

28 **Single and double-stranded DNA have a similar effect on seeded AuNP growth**

1 Various DNA sequences were previously used for directing the growth of AuNSs into
2 different morphologies.^{33, 34} Since the kinetics of DNA adsorption differs significantly
3 between ssDNA and dsDNA,^{1, 35, 36} we wondered if they can produce different growth
4 products. To test this, we incubated a 24-mer random sequenced DNA (24-mer DNA, 100
5 nM) with 0.26 nM AuNSs overnight and then added various concentrations of its
6 complementary DNA (c-24-mer DNA). For the control group, the same concentrations of the
7 24-mer DNA were added, so that only ssDNA was present in the control and its overall DNA
8 concentration was the same as the experiment group (see Figure 1A for the reaction scheme).
9 We then added NH_2OH and HAuCl_4 to both groups to initiate the seeded growth. The
10 solution color varied from purple to blue when the concentration of c-24mer was increased
11 (Figure 1B), which was consistent with the previous report using thiolated DNA.²² However,
12 the same trend was also observed for the control group (Figure 1C). We further plotted their
13 surface plasmon resonance (SPR) peak wavelengths (Figure 1D), which also quantitatively
14 confirmed that the sample and control groups behaved the same. The hybridization of the
15 24-mer and c-24mer was verified by SGI staining (Figure 1E). Thus, the growth was affected
16 by the total DNA concentration but was insensitive to the formation of dsDNA.



1

2 **Figure 1.** (A) Reaction scheme of AuNSs with pre-adsorbed DNA, adding cDNA or
 3 non-complementary DNA, and finally adding HAuCl₄ and NH₂OH to initiate AuNP growth.
 4 UV-vis spectra of AuNPs grown in the presence of 100 nM 24-mer DNA with the addition
 5 of different concentrations of (B) cDNA (c24-mer) and (C) the same sequenced DNA
 6 (24-mer). Insets: photographs showing the color of the corresponding AuNP products. (D)
 7 SPR peak wavelength of the AuNP products with increasing concentration of DNA. (E) The
 8 fluorescence spectra of ssDNA (100 nM 24-mer) and dsDNA (50 nM 24-mer + 50 nM
 9 c24-mer). Inset: fluorescence photograph of the correspondent solutions.

10

11 The above experiments were performed using 100 nM initial DNA concentration. Since
 12 most seeded AuNP growth was performed with 1 μM DNA,³⁷ we also raised the

1 concentration of the DNA to 500 nM and then added up to 500 nM of the c-24mer or 24-mer
2 DNA. In this case, little difference between the sample and control group was observed either,
3 and all of the samples appeared blue due to the higher DNA concentration (Figure S1).

4 Even with just 100 nM DNA, the initial DNA-to-AuNS ratio was 400:1 before adding
5 extra DNA. Since each 13 nm AuNS is expected to adsorb less than 30 DNA
6 oligonucleotides at neutral pH,³⁸ the majority of the DNA strands (>90%) were free in
7 solution. Based on previous research, adsorbed DNA cannot be easily desorbed from AuNPs
8 by its cDNA.^{39, 40} Thus, we only need to consider DNA hybridization in solution. We also
9 switched the order by mixing the DNA with its cDNA first, and then added the AuNSs for the
10 growth reaction (Figure S2A). This way, the difference between ssDNA and dsDNA might
11 be even larger. However, a similar color change and SRP peak shift were still observed for
12 the two groups (Figure S2B-D). All these experiments indicated that AuNP growth was only
13 affected by the total concentration of DNA, and ssDNA and dsDNA behaved similarly. As a
14 result, this method cannot be used for the detection of cDNA.

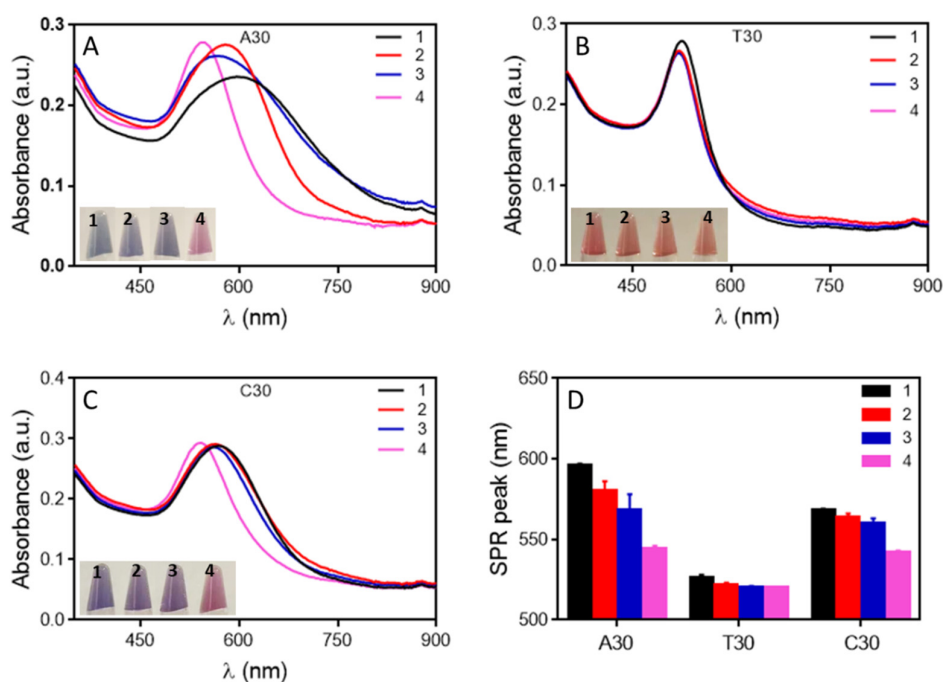
15 **Interaction of H₂AuCl₄ and DNA**

16 Given the difference in the adsorption kinetics of ssDNA and dsDNA to AuNPs,³⁶ one would
17 expect their difference in the seeded growth reaction. However, we did not observe it, and
18 this can be rationalized as follows. Due to the low concentration of the AuNSs, the majority
19 of the DNA (>90% if 100 nM DNA used and >99% if 1 μM DNA used) were free in solution.
20 So, even if 90% of the DNA was hybridized, the remaining 10% ssDNA were still sufficient
21 to saturate the AuNS surface. For comparison, the DNA-to-AuNP ratio was much smaller for
22 typical label-free colorimetric detection (e.g. ~5 nM AuNPs and 20-100 nM probe DNA^{30, 36}),
23 in which case, the formation of dsDNA is more easily probed.

24 In addition, an overlooked reagent in this system might be H₂AuCl₄. In all of the previous
25 work studying DNA-directed seeded growth of AuNPs, only the adsorption of DNA to
26 AuNSs was considered,^{41, 42} while little attention was paid to the potential interactions
27 between H₂AuCl₄ and DNA. Au³⁺ ions can strongly coordinate to various nucleobases and
28 thus affect the property of DNA.⁴³⁻⁴⁵ Herein, we studied the interaction of H₂AuCl₄ with DNA
29 by comparing four ways of mixing and incubation. (1) AuNSs were first mixed with a DNA

1 (A30, T30 or C30) and then NH_2OH and HAuCl_4 were added sequentially. (2) AuNSs were
 2 mixed with a DNA and then HAuCl_4 and NH_2OH were added sequentially. (3) AuNSs were
 3 mixed with a DNA, HAuCl_4 was then added and incubated for 15 min, and finally NH_2OH
 4 was added. (4) A DNA and HAuCl_4 were incubated for 15 min, AuNSs were then added and
 5 incubated for 15 min, and finally NH_2OH was added.

6 For the three DNA sequences, the largest difference between these four mixing methods
 7 was observed with A30 (Figure 2A) followed by C30 (Figure 2C), whereas little difference
 8 was observed with T30 regardless (Figure 2B). This can be attributed to the weaker
 9 interactions between T30 and AuNSs/ HAuCl_4 . The color of the samples was also reflected in
 10 their UV-vis spectra. Therefore, we concluded that a time-dependent interaction between
 11 HAuCl_4 and A30 or C30 existed, and a longer incubation time inhibited the seeded growth
 12 more. It is likely that after an extended incubation, A30 and C30 strongly bound Au^{3+} ions
 13 via their nucleobases to make these bound Au^{3+} ions unavailable for the growth.



14

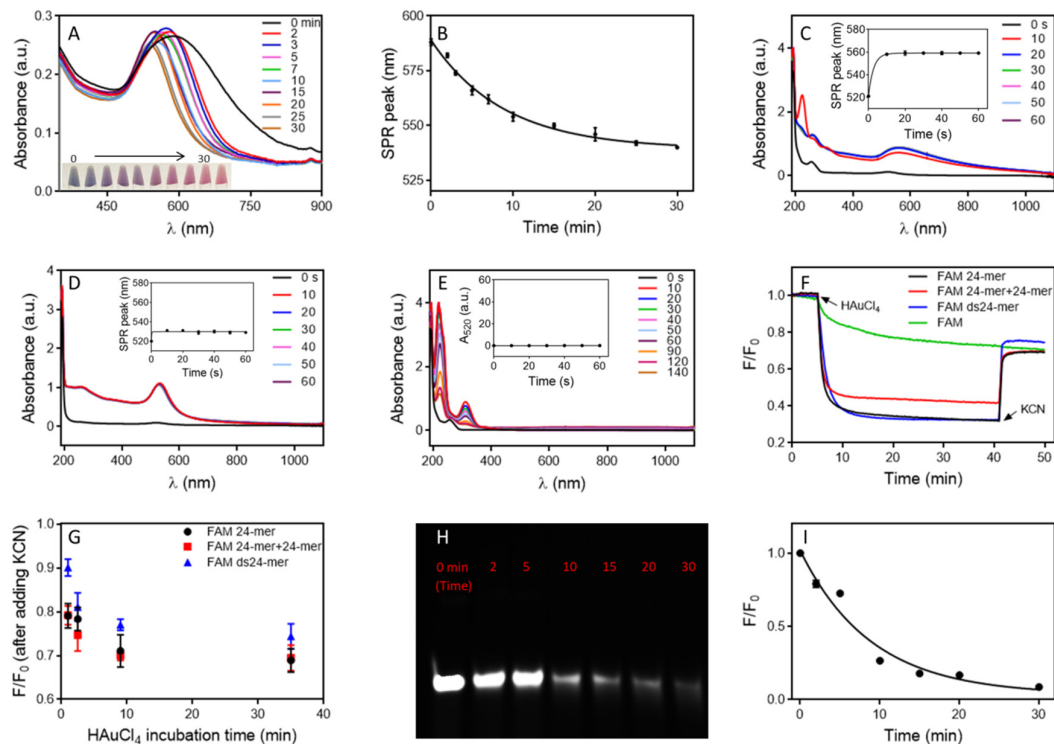
15 **Figure 2.** UV-vis spectra of (A) A30, (B) T30, and (C) C30 directed seeded AuNP growth
 16 with HAuCl_4 added in different orders: (1) AuNSs + DNA, and then NH_2OH and HAuCl_4
 17 added sequentially; (2) AuNSs + DNA and then HAuCl_4 and NH_2OH added sequentially; (3)

1 AuNSs + DNA + H_{AuCl}₄, incubation for 15 min, finally NH₂OH was added; (4) DNA and
2 H_{AuCl}₄ mixed for 15 min, AuNS then added and waited for 15 min, finally NH₂OH added.
3 Insets: photographs of the corresponding AuNPs. (D) Corresponding SPR peak wavelengths
4 of the grown AuNPs in the presence of A30, T30 and C30.

5

6 To further understand the interaction DNA and H_{AuCl}₄ on AuNP growth, we incubated
7 A30 with H_{AuCl}₄ for different times and then added the AuNSs and NH₂OH. The solution
8 color varied from blue to pink accompanied with blue-shifted SPR peaks as the incubation
9 time increased to 30 min (Figure 3A, 3B), confirming that H_{AuCl}₄ reacted with A30 in a
10 time-dependent manner with a fitted first order rate constant of 0.11 min⁻¹. In most
11 DNA-mediated AuNP growth experiments, H_{AuCl}₄ was added the last and the kinetics of the
12 growth reaction was completed in just 10 sec (Figure 3C). In those conditions, the strong
13 interactions between H_{AuCl}₄ and DNA can be negligible. Without DNA, AuNSs can also
14 quickly catalyze the reduction of H_{AuCl}₄ to enlarge the AuNSs (Figure 3D), although the
15 growth was isotropic and the solution remained red. In contrast, for the DNA in solution, the
16 reducing reaction was slower (Figure 3E).

17



1

2 **Figure 3.** (A) UV-vis spectra of A30-directed AuNPs grown with different incubation times
3 of A30 with HAuCl₄. Inset: photographs of the corresponding AuNPs. (B) The SPR peak
4 wavelengths of the AuNPs in (A). (C) UV-vis spectra of A30-directed AuNPs at different
5 growth times. Inset: The corresponding SPR peak wavelengths of the AuNPs. (D) UV-vis
6 spectra of AuNPs grown without DNA at different growth times. Inset: The corresponding
7 SPR peak wavelengths of the AuNPs. (E) UV-vis spectra of A30 directed-AuNP grown
8 without AuNSs at different growth times. Inset: the corresponding absorbance intensity at
9 520 nm of the grown AuNPs. (F) Kinetics of fluorescence change of 100 nM FAM-24mer
10 DNA, and its mixture with 100 nM 24-mer DNA, or with c24-mer DNA to form dsDNA
11 upon adding 167 μM HAuCl₄. The response of free fluorescein dye was also monitored. 20
12 mM KCN was added at 40 min. (G) The relative fluorescent recovery of the samples in (F)
13 after adding KCN to the samples with different HAuCl₄ incubation times. (H) A gel
14 micrograph of 1 μM FAM-A30 incubated with 1 mM of HAuCl₄ in 10 mM PB for different
15 times. (I) The corresponding relative fluorescence intensity in (H), where F₀ presents the
16 initial fluorescence without HAuCl₄

17

1 **Reversible and irreversible Au³⁺/DNA interactions**

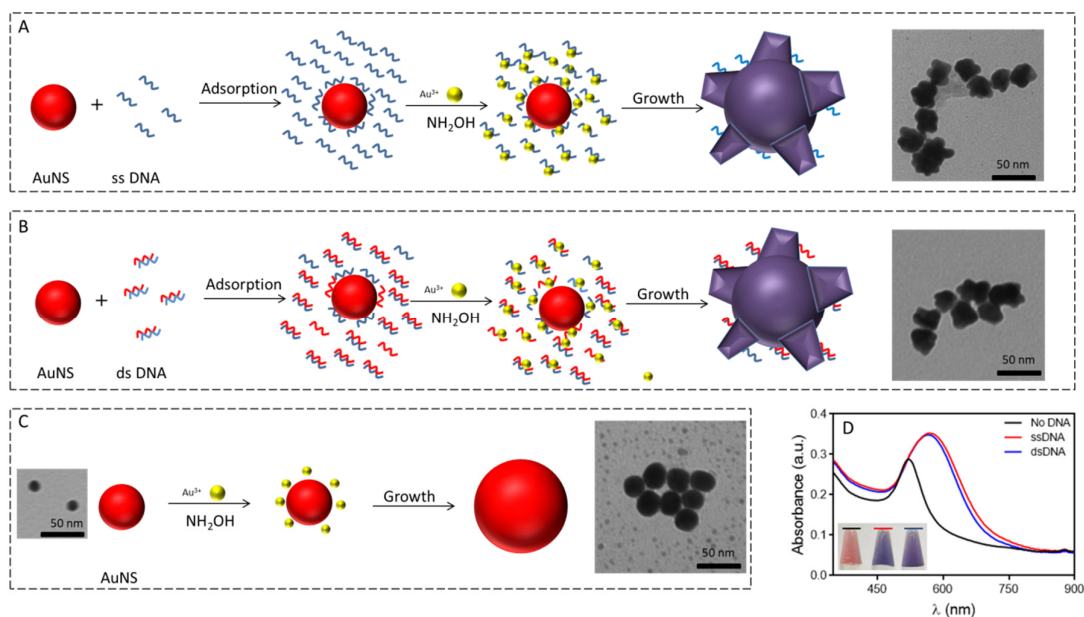
2 To further understand the nature of HAuCl₄ and DNA interactions, we then used a
3 FAM-labeled DNA to monitor the kinetics of fluorescence change (Figure 3F). In addition,
4 we also added its cDNA to probe the effect of dsDNA. Au³⁺ binding to DNA can induce
5 fluorescence quenching. The fluorescence decreased very quickly for all the DNA-containing
6 samples when HAuCl₄ was added (within 1 min). In contrast, the fluorescence dropped
7 slowly for the free fluorescein dye, indicating that the faster drop in the fluorescence was due
8 to HAuCl₄ binding to DNA instead of direct HAuCl₄ interacting with the fluorophore.

9 At 40 min, we added KCN to bind to Au³⁺. When KCN was added, some fluorescence
10 was recovered, suggesting that a fraction of Au³⁺ ions were removed from the DNAs. The
11 unrecovered part can be attributed to very strong and irreversible binding of Au³⁺ to DNA.
12 Some nitrogen atoms in adenine such as N1 and N7 are known to be strong ligand for soft
13 metals such as gold, silver and platinum.⁴³⁻⁴⁵ The longer the DNA/HAuCl₄ incubation time,
14 the lower the fluorescence recovery after adding KCN (Figure S3, Figure 3G). When the
15 HAuCl₄/DNA incubation time was 2 min, 80-90% of fluorescence recovery was observed.
16 Since 2 min is a typical time of adding HAuCl₄ and NH₂OH, HAuCl₄ binding to DNA was
17 still mostly in the weak and reversible state. We reason that the main role of the DNA in
18 solution was to carry HAuCl₄ to the AuNSs. The similarity of ssDNA and dsDNA in
19 interacting with HAuCl₄ may explain their similar effects in directing the growth of AuNPs.

20 The kinetics in Figure 3B and Figure 3F were comparable, and both measured the effect
21 of long-time incubation of DNA with HAuCl₄. To confirm irreversible HAuCl₄/DNA
22 interactions, we incubated FAM-A30 DNA with HAuCl₄ for various times and
23 concentrations, and then analyzed the products using gel electrophoresis (Figure 3H and 3I,
24 Figure S4). The intensity of the FAM-A30 band gradually decreased indicating that the
25 irreversible HAuCl₄/FAM-A₃₀ product was highly stable and it survived the denaturing gel
26 electrophoresis.

27 Based on the above results, we described the DNA-directed seeded growth in Figure 4. A
28 key role of DNA is to recruit Au³⁺ ions to the surface of AuNSs. Without DNA, a lot of small

1 AuNPs were observed in the background of the enlarged AuNPs (Figure 4C), indicating Au³⁺
 2 ions in solution can also be reduced outside the AuNSs. When DNA was present, the
 3 background was clean (Figure 4A and 4B), which may be attributed to the DNA binding to
 4 HAuCl₄ inhibiting nucleation. In this regard, the kinetics and capacity of ssDNA and dsDNA
 5 binding to HAuCl₄ were similar and it may explain why they showed little difference in the
 6 growth reaction. The sequence of DNA determines the morphology outcomes, which is
 7 related to their selective adsorption to certain golds facets.^{41, 46, 47} The AuNSs also catalyzed
 8 the reduction of Au³⁺ (this has been commonly used for the growth of silver⁴⁸), and thus the
 9 Au³⁺ ions near the AuNS surface were more easily reduced and deposited. While free ssDNA
 10 and dsDNA had a large difference in adsorption kinetics on AuNPs, under the seeded growth
 11 condition (e.g., a great excess of DNA and similar binding to HAuCl₄), the difference was
 12 smaller.



13

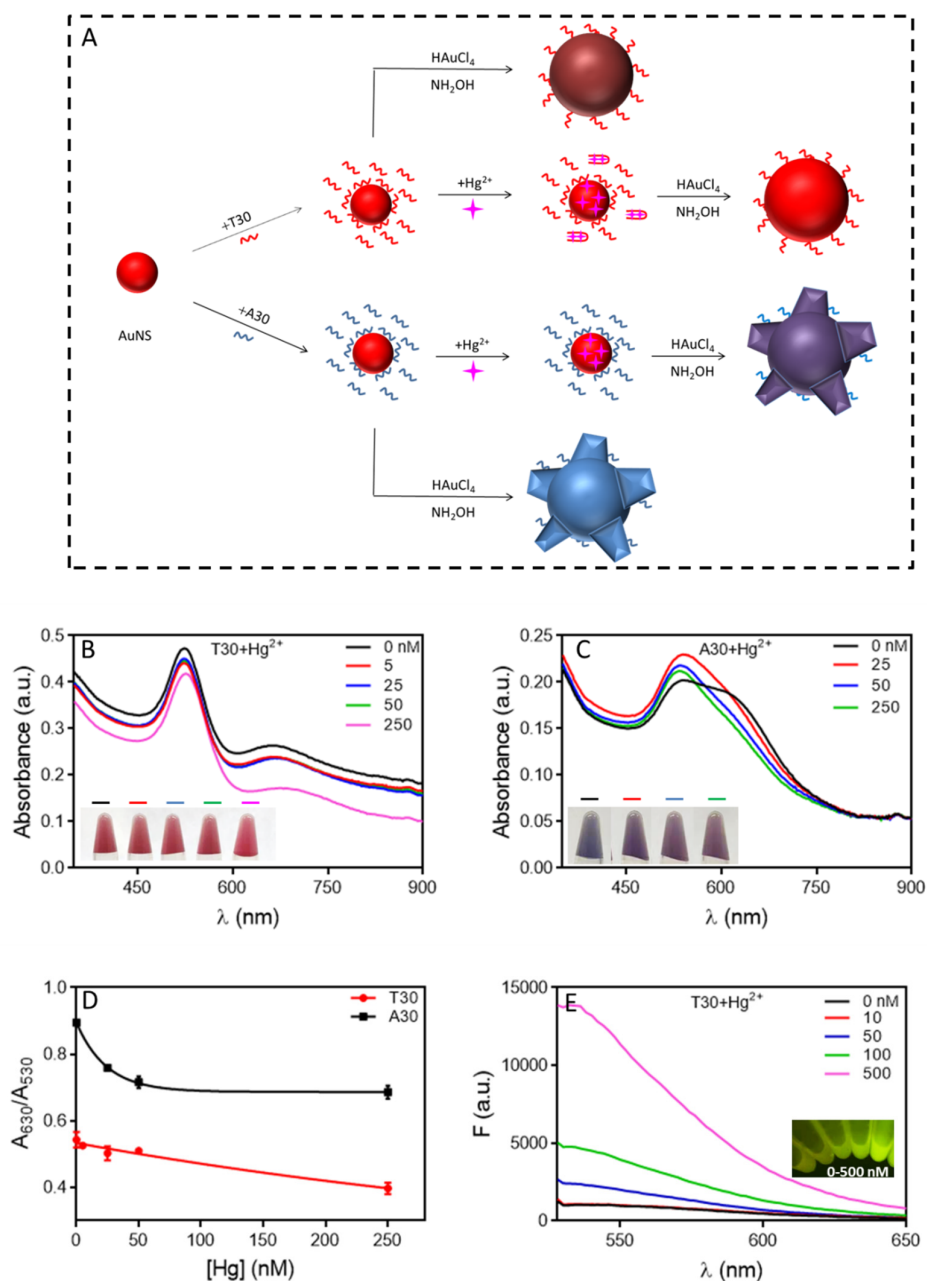
14 **Figure 4.** Reaction scheme of (A) ssDNA, (B) dsDNA, and (C) no DNA directed AuNP
 15 growth. Note that the DNA is in great excess. Even for a dsDNA sample, likely some free
 16 ssDNA strands still exist to adsorb to the AuNSs. (D) UV-vis spectra of ssDNA, dsDNA and
 17 no DNA-coated AuNPs after the seeded growth. Insets: photographs of the corresponding
 18 AuNPs.

19

1 **Hg²⁺ detection effect using Aptamer-AuNP**

2 The above work compared ssDNA and dsDNA directed seeded growth, and indicated that the
3 growth cannot be used for label-free detection of cDNA. We then studied a few aptamer
4 targets and started with Hg²⁺ (Figure 5A). Hg²⁺/AuNP interactions are well known,^{12, 49}
5 which may play a role. We chose T30 DNA as a probe for Hg²⁺ taking advantage of the
6 T-Hg²⁺-T interaction. The optimal concentration of T30 was determined to be 1 μM, since
7 further increase of the DNA concentration did not induce more peak shift (Figure S5). We
8 respectively incubated T30 and A30 with AuNSs overnight and then added different
9 concentrations of Hg²⁺ followed by the growth procedures. As shown in Figure 5B, for the
10 T30 sample, the solution color changed only slightly from dark red to light red and the
11 A₆₃₀/A₅₃₀ ratio decreased only around 0.1 as the concentration of Hg²⁺ increased (Figure 5D).
12 Under TEM, the T30 treated AuNPs appeared to be enlarged spherical nanoparticles (Figure
13 S6). This decreasing trend was consistent with the previous literature report, where T15 was
14 used.¹²

15 We also used A30 DNA as a control sample, where the solution color changed from blue
16 to purple (Figure 5C). The more obvious color change was due to the use of poly-A sequence.
17 The A₆₃₀/A₅₃₀ ratio also decreased, and the decrease was even larger than that of the T30
18 samples, indicating both the A30 and T30 samples had similar responses to Hg²⁺. In fact, the
19 limit of detection with A30 (1.2 nM) was even lower than that with T30 (12.8 nM). The
20 binding of Hg²⁺ by T30 was confirmed by the fluorescence enhancement of SGI (Figure 5E,
21 Figure S7).⁵⁰ Therefore, based on the decreasing trend of the A₆₃₀/A₅₃₀ ratio, one cannot
22 conclude that Hg²⁺ binding to T30 DNA was responsible for its color change. Hg²⁺
23 adsorption to AuNPs can increase the colloidal stability of AuNPs,¹² and the reason for
24 Hg²⁺-dependent color change could be related to Hg²⁺ adsorption to AuNPs or Hg²⁺ binding
25 to the DNA in solution.



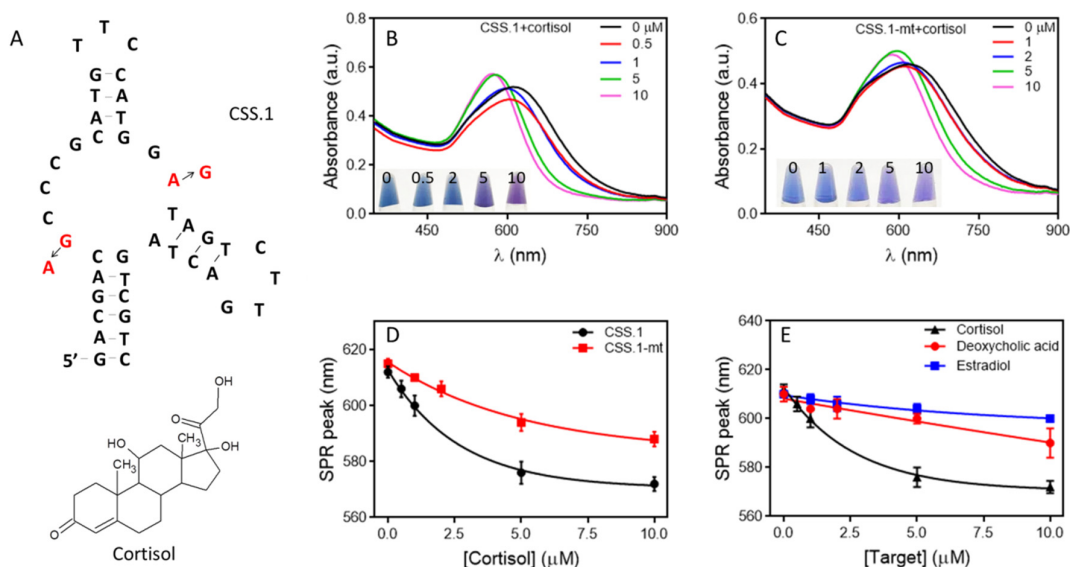
1

2 **Figure 5.** (A) Reaction scheme of growth of AuNPs with T30 or A30 DNA without or with
 3 Hg²⁺. UV-vis absorption spectra of AuNPs grown with (B) T30 and (C) A30 in the presence
 4 of Hg²⁺. Insets: photograph showing the corresponding color of the AuNP products. (D) The
 5 extinction ratio of the AuNP samples in (B, C). The final DNA concentration was 1 μM. (E)
 6 The fluorescence emission spectrum of T30 DNA with different Hg²⁺ concentrations stained
 7 with SGI. Inset: the photograph of the correspondent solutions.

8

1 **Cortisol detection**

2 Since Hg^{2+} can interact with both AuNPs and DNA, it is difficult to obtain mechanistic
3 insights. Small molecules such as cortisol and quinine were then studied. A cortisol aptamer
4 (CSS.1) reported by the Stojanovic group was used (Figure 6A),⁵¹ and we previously reported
5 that cortisol does not have strong interactions with AuNPs.⁵² The optimal concentration of
6 aptamer was determined to be 500 nM (Figure S8), where the slope started to plateau and the
7 solution color turned blue. In addition, a nonbinding mutant (CSS.1-mt) was also used. Both
8 DNA strands were incubated with the AuNSs overnight, and then different concentrations of
9 cortisol were mixed followed by the growth procedures. As shown in Figure 6B-E, for the
10 CSS.1 sample, an increase in target concentration caused a color change from blue to purple
11 and blue-shifted SPR peak. The final morphology of the AuNPs was flower-like (Figure S9).
12 For the CSS.1-mt sample, the same trend was observed, but the amount of the peak shift was
13 smaller. Based on Figure 6D, we calculated the limit of detection to be 0.5 μM and 1.3 μM
14 for the CSS.1 aptamer and the mutant, respectively. Since the difference in the aptamer and
15 the mutant was quite small, this is not a good detection method. We then tested the selectivity
16 of this sensor by using 17β -estradiol and deoxycholic acid (Figure 6E and S10), which had a
17 less influence on the growth compared with cortisol. Therefore, cortisol binding to its
18 aptamer can be reflected by this reaction.



19

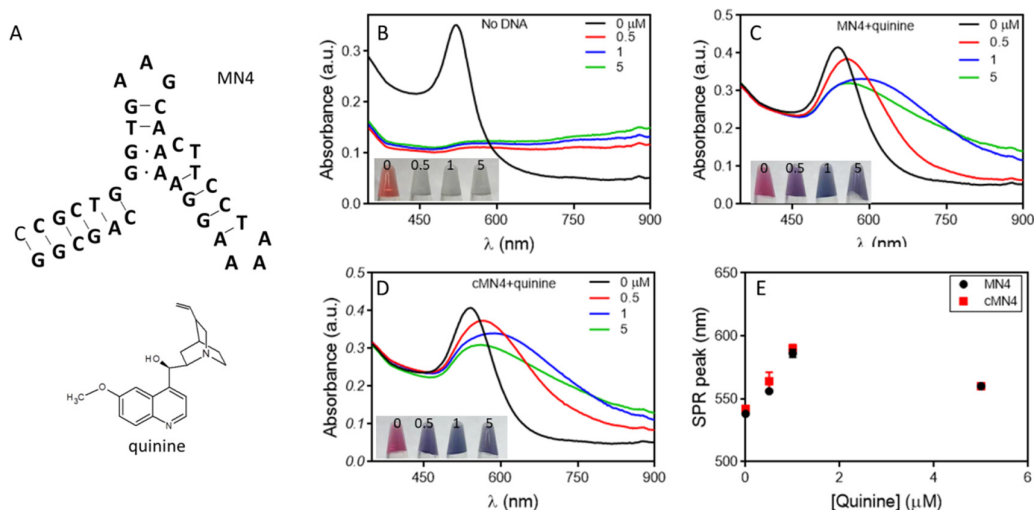
1 **Figure 6.** The secondary structure of the cortisol aptamer (CSS.1) and the structure of
 2 cortisol. The two mutated bases in CSS.1-mt are shown in red. UV-vis spectra of AuNPs
 3 grown with (B) CSS.1 and (C) the mutated aptamer (CSS.1-mt) with different concentrations
 4 of cortisol. Inset: photographs of the samples. The final aptamer concentration was 500 nM.
 5 (D) SPR peak wavelength of the AuNPs grown with increasing concentrations of cortisol. (E)
 6 SPR peak wavelengths of the AuNPs grown with increasing concentrations of cortisol,
 7 17 β -estradiol or deoxycholic acid.

8

9 **Quinine detection**

10 Finally, we also tested the detection of quinine using its aptamer called MN4 (Figure 7A).
 11 The optimal aptamer concentration was determined to be 500 nM (Figure S11). For both
 12 MN4 and the control sequence (we used its cDNA named c-MN4 in this case), a color change
 13 from red to blue and a redshift in the SPR peak were observed as the concentration of quinine
 14 was increased from 0 to 1 μ M. With further increase of quinine to 5 μ M, the SPR peak then
 15 blue-shifted (Figure 7C-E). The morphologies of the growth products were both nanoflowers
 16 (Figure S12). Since the aptamer and the control behaved exactly the same, this method cannot
 17 be used for the detection of quinine. This might be related to the strong adsorption of quinine
 18 to AuNPs leading to its aggregation (Figure 7B).²⁷

19



20

1 **Figure 7.** (A) The secondary structure of the quinine aptamer (MN4) and the structure of
2 quinine. UV-vis spectra of the AuNPs (B) without DNA and without the growth reaction, (C)
3 grown with MN4 and (D) grown with cMN4 with the addition of different concentrations of
4 quinine. Insets: photographs showing the color of the corresponding AuNPs. The final
5 aptamer concentration was 500 nM. (E) SPR peak wavelengths of the corresponding AuNPs
6 grown with increasing concentrations of quinine.

8 **Different types of aptamer targets**

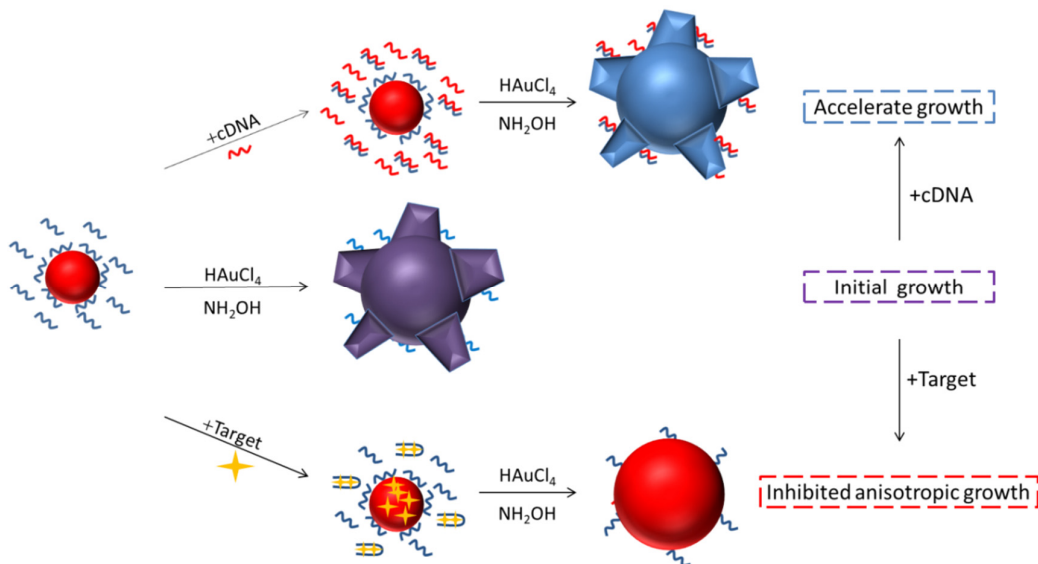
9 The seeded growth reaction was previously used to detect a few aptamer targets including
10 Hg^{2+} , ochratoxin A, cocaine and 17β -estradiol. We herein tested three additional targets in
11 this paper. We summarized the experimental details between the previous studies and our
12 study in Table S1, and the conditions were quite comparable. We classified target analytes
13 into a few types. In the case of ochratoxin A and cortisol, their aptamers showed a better
14 response compared to the non-binding control sequences, and the seeded growth reactions
15 were likely to be able to reflect the aptamer binding reactions. That being said, the practical
16 use of this reaction is unlikely due to potential interferences such as extra DNA present in the
17 system. For analytes like Hg^{2+} that can adsorb to and stabilize AuNPs, their aptamers had no
18 obvious advantage compared to non-aptamer sequences. For analytes like quinine leading to
19 aggregation of AuNPs, and aptamers had no difference compared to the control sequences
20 either. Overall, this growth reaction is unlikely to be a practically useful detection platform
21 for aptamer binding.

22

23 **Opposite colorimetric results of DNA and aptamer based detection**

24 Normally, one would expect DNA and aptamer targets to have the same sensor phenomena
25 since cDNA can be considered as a special aptamer target. In this seeded growth case,
26 however, the trends of color change were different. For cDNA detection, the more cDNA
27 added, the more blue color, while for aptamer target detection, the more targets, the more red
28 color. As demonstrated in this work, the main difference is anisotropic growth directed by
29 DNA versus isotropic growth without DNA (or with poly-T DNA). DNA can promote
30 anisotropic growth and thus color change to blue, and the added cDNA can also contribute to

1 it. On the other hand, aptamer binding to its target and target adsorption both would inhibit
 2 aptamer adsorption without changing the overall DNA concentration in the system,
 3 explaining the red color outcome. We summarized the difference between DNA and aptamer
 4 probes in Figure 8.



5

6 **Figure 8.** Reaction schemes of grown DNA-coated AuNPs in the presence or absence of
 7 cDNA or target.

8

9 **Conclusions**

10 In this work, we carefully studied the seeded growth reaction and evaluated its application to
 11 detect DNA and aptamer targets. We found that this reaction cannot be used for the detection
 12 of DNA hybridization. The reason is that both ssDNA and dsDNA can promote the growth of
 13 AuNPs similarly due to their similar weak reversible adsorption mode of HAuCl₄ under the
 14 growth condition. Therefore, adding cDNA or a random sequenced DNA would produce a
 15 similar promotion effect on the growth reaction. Compared to other DNA/AuNP sensing
 16 systems, the seeded growth system has a much higher DNA/AuNS ratio and thus a high
 17 concentration of free DNA, which also makes it difficult to detect cDNA. Aptamer targets, on
 18 the other hand, can bind to aptamers to inhibit aptamer adsorption and/or adsorb to AuNSs to
 19 inhibit aptamer adsorption, both of which can inhibit the growth reaction. Therefore, DNA
 20 targets and aptamer targets have an opposite effect on the growth reaction. Not all aptamer
 21 targets can be detected due to various reasons such as aggregation of AuNPs as seen in the

1 case of quinine, and increased colloidal stability of AuNPs in the case of Hg²⁺. Overall, using
2 this method to develop colorimetric biosensors is not recommended, but this can be an
3 interesting reaction to understand the interactions of aptamer targets and AuNPs.

4 5 **Acknowledgements**

6 Funding for this work was from the Natural Sciences and Engineering Research Council of
7 Canada (NSERC) and the National Natural Science Foundation of China (31901776 and
8 32072181). C. Lu was supported by a China Scholarship Council (CSC) scholarship to visit
9 the University of Waterloo.

10 11 **Reference**

12 (1) Liu, B.; Liu, J., Interface-Driven Hybrid Materials Based on DNA-Functionalized Gold
13 Nanoparticles. *Matter* **2019**, 1, 825-847.

14 (2) Liu, J., Adsorption of DNA onto Gold Nanoparticles and Graphene Oxide: Surface
15 Science and Applications. *Physical chemistry chemical physics : PCCP* **2012**, 14, 10485-96.

16 (3) Zhang, X.; Servos, M. R.; Liu, J., Surface Science of DNA Adsorption onto
17 Citrate-Capped Gold Nanoparticles. *Langmuir* **2012**, 28, 3896-902.

18 (4) Farkhari, N.; Abbasian, S.; Moshaii, A.; Nikkhah, M., Mechanism of Adsorption of
19 Single and Double Stranded DNA on Gold and Silver Nanoparticles: Investigating Some
20 Important Parameters in Bio-Sensing Applications. *Colloids Surf. B Biointerfaces* **2016**, 148,
21 657-664.

22 (5) Hu, S.; Huang, P. J.; Wang, J.; Liu, J., Dissecting the Effect of Salt for More Sensitive
23 Label-Free Colorimetric Detection of DNA Using Gold Nanoparticles. *Anal. Chem.* **2020**, 92,
24 13354-13360.

25 (6) Sarfraz, N.; Khan, I., Plasmonic Gold Nanoparticles (AuNPs): Properties, Synthesis and
26 Their Advanced Energy, Environmental and Biomedical Applications. *Chem. Asian J.* **2021**,
27 16, 720-742.

28 (7) Chen, J.; Ma, Y.; Du, W.; Dai, T.; Wang, Y.; Jiang, W.; Wan, Y.; Wang, Y.; Liang, G.;
29 Wang, G., Furin-Instructed Intracellular Gold Nanoparticle Aggregation for Tumor
30 Photothermal Therapy. *Adv. Funct. Mater.* **2020**, 30, 2001566.

- 1 (8) Wu, K.; Li, T.; Schmidt, M. S.; Rindzevicius, T.; Boisen, A.; Ndoni, S., Gold
2 Nanoparticles Sliding on Recyclable Nanohoods—Engineered for Surface-Enhanced
3 Raman Spectroscopy. *Adv. Funct. Mater.* **2018**, 28, 1704818.
- 4 (9) Hizir, M. S.; Top, M.; Balcioglu, M.; Rana, M.; Robertson, N. M.; Shen, F.; Sheng, J.;
5 Yigit, M. V., Multiplexed Activity of Peroxidase: DNA-Capped AuNPs Act as Adjustable
6 Peroxidase. *Anal. Chem.* **2016**, 88, 600-605.
- 7 (10) Sharma, T. K.; Ramanathan, R.; Weerathunge, P.; Mohammadtaheri, M.; Daima, H. K.;
8 Shukla, R.; Bansal, V., Aptamer-Mediated ‘Turn-Off/Turn-on’ Nanozyme Activity of Gold
9 Nanoparticles for Kanamycin Detection. *Chem. Commun.* **2014**, 50, 15856-15859.
- 10 (11) Huang, P.-J. J.; Yang, J.; Chong, K.; Ma, Q.; Li, M.; Zhang, F.; Moon, W. J.; Zhang, G.;
11 Liu, J., Good's Buffers Have Various Affinities to Gold Nanoparticles Regulating Fluorescent
12 and Colorimetric DNA Sensing. *Chem. Sci.* **2020**, 11, 6795-6804.
- 13 (12) Hu, Y.; Huang, Z.; Liu, B.; Liu, J., Hg (II) Adsorption on Gold Nanoparticles Dominates
14 DNA-Based Label-Free Colorimetric Sensing. *ACS Appl. Nano Mater.* **2021**, 4, 1377-1384.
- 15 (13) He, Q.; Wu, Q.; Feng, X.; Liao, Z.; Peng, W.; Liu, Y.; Peng, D.; Liu, Z.; Mo, M.,
16 Interfacing DNA with Nanoparticles: Surface Science and Its Applications in Biosensing. *Int.*
17 *J. Biol. Macromol.* **2020**, 151, 757-780.
- 18 (14) Liu, X.; He, F.; Zhang, F.; Zhang, Z.; Huang, Z.; Liu, J., Dopamine and Melamine
19 Binding to Gold Nanoparticles Dominates Their Aptamer-Based Label-Free Colorimetric
20 Sensing. *Anal. Chem.* **2020**, 92, 9370-9378.
- 21 (15) Lu, C.; Zhou, S.; Gao, F.; Lin, J.; Liu, J.; Zheng, J., DNA-Mediated Growth of Noble
22 Metal Nanomaterials for Biosensing Applications. *TrAC Trends Anal. Chem.* **2022**, 148,
23 116533.
- 24 (16) Zhang, L.; Ma, X. Y.; Wang, G. Q.; Liang, X. G.; Mitomo, H.; Pike, A.; Houlton, A.;
25 Ijiro, K., Non-Origami DNA for Functional Nanostructures: From Structural Control to
26 Advanced Applications. *Nano Today* **2021**, 39, 101154.
- 27 (17) Lu, C.; Tang, L.; Gao, F.; Li, Y.; Liu, J.; Zheng, J., DNA-Encoded Bimetallic Au-Pt
28 Dumbbell Nanozyme for High-Performance Detection and Eradication of Escherichia Coli
29 O157:H7. *Biosens. Bioelectron.* **2021**, 187, 113327.

- 1 (18) Satyavolu, N. S. R.; Loh, K. Y.; Tan, L. H.; Lu, Y., Discovery of and Insights into DNA
2 "Codes" for Tunable Morphologies of Metal Nanoparticles. *Small* **2019**, 15, e1900975.
- 3 (19) Peng, T.; Li, X.; Li, K.; Nie, Z.; Tan, W., DNA-Modulated Plasmon Resonance:
4 Methods and Optical Applications. *ACS Appl. Mater. Interfaces* **2020**, 12, 14741-14760.
- 5 (20) Wang, Y.; Satyavolu, N. S. R.; Lu, Y., Sequence-Specific Control of Inorganic
6 Nanomaterials Morphologies by Biomolecules. *Curr. Opin. Colloid Interface Sci.* **2018**, 38,
7 158-169.
- 8 (21) Lu, C.; Zandieh, M.; Zheng, J.; Liu, J., DNA-Directed Seeded Synthesis of Gold
9 Nanoparticles without Changing DNA Sequence. *ChemNanoMat* **2022**, 8, e202200111.
- 10 (22) Fang, W. F.; Chen, W. J.; Yang, J. T., Colorimetric Determination of DNA
11 Concentration and Mismatches Using Hybridization-Mediated Growth of Gold Nanoparticle
12 Probes. *Sens. Actuators B Chem.* **2014**, 192, 77-82.
- 13 (23) Wang, H. Q.; Rao, H. H.; Luo, M. Y.; Xue, X.; Xue, Z. H.; Lu, X. Q., Noble Metal
14 Nanoparticles Growth-Based Colorimetric Strategies: From Monocolorimetric to
15 Multicolorimetric Sensors. *Coordin. Chem. Rev.* **2019**, 398, 113003.
- 16 (24) Li, N.; Liu, S. G.; Zhu, Y. D.; Liu, T.; Lin, S. M.; Shi, Y.; Luo, H. Q.; Li, N. B., Tuning
17 Gold Nanoparticles Growth Via DNA and Carbon Dots for Nucleic Acid and Protein
18 Detection. *Sens. Actuators B Chem* **2017**, 251, 455-461.
- 19 (25) Tan, L.; Chen, Z.; Zhang, C.; Wei, X.; Lou, T.; Zhao, Y., Colorimetric Detection of Hg²⁺
20 Based on the Growth of Aptamer-Coated Aunps: The Effect of Prolonging Aptamer Strands.
21 *Small* **2017**, 13.
- 22 (26) Soh, J. H.; Lin, Y.; Rana, S.; Ying, J. Y.; Stevens, M. M., Colorimetric Detection of
23 Small Molecules in Complex Matrixes Via Target-Mediated Growth of
24 Aptamer-Functionalized Gold Nanoparticles. *Anal. Chem.* **2015**, 87, 7644-52.
- 25 (27) Zhang, F.; Liu, J., Interactions of the Cocaine and Quinine Aptamer with Gold
26 Nanoparticles under the Dilute Biosensor and Concentrated Nmr Conditions. *Langmuir* **2021**,
27 37, 11939-11947.
- 28 (28) Lopez, A.; Liu, J., Nanomaterial and Aptamer-Based Sensing: Target Binding Versus
29 Target Adsorption Illustrated by the Detection of Adenosine and Atp on Metal Oxides and
30 Graphene Oxide. *Anal. Chem.* **2021**, 93, 3018-3025.

- 1 (29)Zhou, J.; Li, Y.; Wang, W.; Lu, Z.; Han, H.; Liu, J., Kanamycin Adsorption on Gold
2 Nanoparticles Dominates Its Label-Free Colorimetric Sensing with Its Aptamer. *Langmuir*
3 **2020**, 36, 11490-11498.
- 4 (30)Zhang, F.; Liu, J., Label-Free Colorimetric Biosensors Based on Aptamers and Gold
5 Nanoparticles: A Critical Review. *Anal. Sens.* **2021**, 1, 30-43.
- 6 (31)Zhang, F.; Huang, P.-J. J.; Liu, J., Sensing Adenosine and Atp by Aptamers and Gold
7 Nanoparticles: Opposite Trends of Color Change from Domination of Target Adsorption
8 Instead of Aptamer Binding. *ACS Sens.* **2020**, 5, 2885-2893.
- 9 (32)Liu, J.; Lu, Y., Preparation of Aptamer-Linked Gold Nanoparticle Purple Aggregates for
10 Colorimetric Sensing of Analytes. *Nat. Protoc.* **2006**, 1, 246-52.
- 11 (33)Reddy Satyavolu, N. S.; Pishvaresfahani, N.; Tan, L. H.; Lu, Y., DNA-Encoded
12 Morphological Evolution of Bimetallic Pd@Au Core-Shell Nanoparticles from a
13 High-Indexed Core. *Nano Res.* **2018**, 11, 4549-4561.
- 14 (34)Tan, L. H.; Yue, Y.; Satyavolu, N. S.; Ali, A. S.; Wang, Z.; Wu, Y.; Lu, Y., Mechanistic
15 Insight into DNA-Guided Control of Nanoparticle Morphologies. *J. Am. Chem. Soc.* **2015**,
16 137, 14456-64.
- 17 (35)Li, F.; Pei, H.; Wang, L.; Lu, J.; Gao, J.; Jiang, B.; Zhao, X.; Fan, C., Nanomaterial-
18 Based Fluorescent DNA Analysis: A Comparative Study of the Quenching Effects of
19 Graphene Oxide, Carbon Nanotubes, and Gold Nanoparticles. *Adv. Funct. Mater.* **2013**, 23,
20 4140-4148.
- 21 (36)Li, H.; Rothberg, L. J., Label-Free Colorimetric Detection of Specific Sequences in
22 Genomic DNA Amplified by the Polymerase Chain Reaction. *J. Am. Chem. Soc.* **2004**, 126,
23 10958-10961.
- 24 (37)Wang, Z.; Zhang, J.; Ekman, J. M.; Kenis, P. J.; Lu, Y., DNA-Mediated Control of Metal
25 Nanoparticle Shape: One-Pot Synthesis and Cellular Uptake of Highly Stable and Functional
26 Gold Nanoflowers. *Nano Lett.* **2010**, 10, 1886-91.
- 27 (38)Zhang, X.; Liu, B.; Dave, N.; Servos, M. R.; Liu, J., Instantaneous Attachment of an
28 Ultrahigh Density of Nonthiolated DNA to Gold Nanoparticles and Its Applications.
29 *Langmuir* **2012**, 28, 17053-17060.

- 1 (39)Herne, T. M.; Tarlov, M. J., Characterization of DNA Probes Immobilized on Gold
2 Surfaces. *J. Am. Chem. Soc.* **1997**, 119, 8916-8920.
- 3 (40)Zhang, F.; Wang, S.; Liu, J., Gold Nanoparticles Adsorb DNA and Aptamer Probes Too
4 Strongly and a Comparison with Graphene Oxide for Biosensing. *Anal. Chem.* **2019**, 91,
5 14743-14750.
- 6 (41)Wang, Z.; Tang, L.; Tan, L. H.; Li, J.; Lu, Y., Discovery of the DNA “Genetic Code” for
7 Abiological Gold Nanoparticle Morphologies. *Angew. Chem. Int. Ed.* **2012**, 51, 9078-9082.
- 8 (42)Song, T.; Tang, L.; Tan, L. H.; Wang, X.; Satyavolu, N. S.; Xing, H.; Wang, Z.; Li, J.;
9 Liang, H.; Lu, Y., DNA-Encoded Tuning of Geometric and Plasmonic Properties of
10 Nanoparticles Growing from Gold Nanorod Seeds. *Angew. Chem. Int. Ed.* **2015**, 54, 8114-8.
- 11 (43)Lopez, A.; Liu, J., Coordination Nanoparticles Formed by Fluorescent 2-Aminopurine
12 and Au³⁺: Stability and Nanozyme Activities. *J. Anal. Test.* **2019**, 3, 219-227.
- 13 (44)Yoshimoto, T.; Seki, M.; Okabe, H.; Matsuda, N.; Wu, D.-y.; Futamata, M., Three
14 Distinct Adsorbed States of Adenine on Gold Nanoparticles Depending on pH in Aqueous
15 Solutions. *Chem. Phys. Lett.* **2022**, 786, 139202.
- 16 (45)Verma, S.; Mishra, A. K.; Kumar, J., The Many Facets of Adenine: Coordination,
17 Crystal Patterns, and Catalysis. *Acc. Chem. Res.* **2009**, 43, 79-91.
- 18 (46)Tan, L. H.; Xing, H.; Lu, Y., DNA as a Powerful Tool for Morphology Control, Spatial
19 Positioning, and Dynamic Assembly of Nanoparticles. *Acc. Chem. Res.* **2014**, 47, 1881-90.
- 20 (47)Tan, L. H.; Xing, H.; Chen, H.; Lu, Y., Facile and Efficient Preparation of Anisotropic
21 DNA-Functionalized Gold Nanoparticles and Their Regioselective Assembly. *J. Am. Chem.*
22 *Soc.* **2013**, 135, 17675-17678.
- 23 (48)Taton, T. A.; Mirkin, C. A.; Letsinger, R. L., Scanometric DNA Array Detection with
24 Nanoparticle Probes. *Science* **2000**, 289, 1757-1760.
- 25 (49)Schmidbaur, H.; Schier, A., Auophilic Interactions as a Subject of Current Research: An
26 up-Date. *Chem. Soc. Rev.* **2012**, 41, 370-412.
- 27 (50)Wang, J.; Liu, B., Highly Sensitive and Selective Detection of Hg²⁺ in Aqueous Solution
28 with Mercury-Specific DNA and Sybr Green I. *Chem. Commun.* **2008**, 4759-4761.

1 (51)Yang, K.-A.; Chun, H.; Zhang, Y.; Pecic, S.; Nakatsuka, N.; Andrews, A. M.; Worgall, T.
2 S.; Stojanovic, M. N., High-Affinity Nucleic-Acid-Based Receptors for Steroids. *ACS Chem.*
3 *Biol.* **2017**, 12, 3103-3112.

4 (52)Niu, C.; Ding, Y.; Zhang, C.; Liu, J., Comparing Two Cortisol Aptamers for Label-Free
5 Fluorescent and Colorimetric Biosensors. *Sensors & Diagnostics* **2022**,1, 541-549.

6

7